Mechanics of Materials 26 (1997) 63–80

MECHANICS OF MATERIALS

On the Use of Shear-Lag Methods for Analysis of Stress Transfer in Unidirectional Composites

John A. Nairn*

Material Science and Engineering, 304 EMRO Bldg., University of Utah, Salt Lake City, Utah 84112, USA

Received 6 November 1996

Abstract

The "shear-lag" analysis method is frequently used for analysis of stress transfer between the fiber and the matrix in composites. The accuracy of shear-lag methods has not been critically assessed, in part because the assumptions have not been fully understood. This paper starts from the exact equations of elasticity for axisymmetric stress states in transversely isotropic materials and introduces the minimum assumptions required to derive the most commonly used shear-lag equations. These assumptions can now be checked to study the accuracy of shear-lag analysis on any problem. Some sample calculations were done for stress transfer from a matrix into a broken fiber. The shear-lag method did a reasonable job (within 20%) of predicting average axial stress in the fiber and total strain energy in the specimen provided the shear-lag parameter most commonly used in the literature is replaced by a new one derived from the approximate elasticity analysis. The shear-lag method does a much worse job of predicting shear stresses and energy release rates. Furthermore, the shear-lag method does not work for low fiber volume fractions.

1. Introduction

The so-called "shear lag" method is often used for analysis of stress transfer problems in composites. The term "shear lag" can be traced, prior to its use in composites, to analysis of bending of I beams and T beams with wide flanges (Troitsky, 1976) and to box beams (Reissner, 1946). Simple beam theory predicts that the axial displacements in the flanges of such beams are only a function of the distance from the neutral axis and independent of the distance from the web. This simple theory also predicts zero shear stress and zero shear strain in the flange. In reality, the true axial displacements "lag" behind the beam theory predictions. This "lag" is cause by load diffusion which can be viewed (using equilibrium arguments) as a consequence of non-zero shear stresses in the flange — hence the term "shear lag." In these beam analyses, "shear lag" is an effect and not an analysis method. Many possible analysis methods can evaluate the "shear lag" effect. These methods generally result in defining an *effective* flange width that is less than the actual flange width (Troitsky, 1976). If effective width is not considered when designing beams, the resulting beams can be seriously under designed.

In composites, the term "shear lag" is associated with a stress transfer analysis method originally proposed by Cox (1952) as a small part of a larger paper on the elasticity and strength of fibrous materials. He derived a one-dimensional equation for fiber stress that can be written as

$$\frac{\partial^2 \langle\sigma_f\rangle}{\partial z^2} - \beta^2 \langle\sigma_f\rangle = -\beta^2 \langle\sigma_{f\infty}\rangle \tag{1}$$

*Tel.: +1-801-5813413; fax: +1-801-5814816; e-mail: john.nairn@m.cc.utah.edu.

 Author prepared reprint.

where $\langle\sigma_f\rangle$ is the average axial stress in the fiber, $\langle\sigma_{f\infty}\rangle$ is the average axial stress in the corresponding infinitely long fiber embedded in an infinitely long matrix, and β is the shear lag parameter. Cox (1952) further stated that the shear-lag parameter is given by

$$\beta = \beta_{\rm COX} = \frac{1}{r_1}\sqrt{\frac{2G_m}{E_f \ln\frac{s}{r_1}}} \tag{2}$$

where G_m is the matrix shear modulus, E_f is the fiber axial modulus, r_1 is the fiber radius, and s is the mean center-to-center separation of fibers normal to their length (Cox, 1952). When Cox's model is applied to concentric cylinders with the fiber as the central cylinder, s is generally taken as equal to r_2 or the outer radius of the matrix cylinder (Piggott, 1987); that convention, because it is the predominant convention, will be used in this paper. A more literal interpretation Cox's analysis might use $s = 2r_2$.

Cox (1952) derived Eq. (1) by starting with an exact equilibrium relation between average fiber stress, $\langle\sigma_f\rangle$, and interfacial shear stress, τ:

$$\frac{\partial\langle\sigma_f\rangle}{\partial z} = -\frac{2\tau}{r_1} \tag{3}$$

Equation 3 follows by integrating the axial equation of stress equilibrium over the fiber cross-sectional area (McCartney, 1992). To eliminate shear stress, Cox (1952) introduced the assumption that

$$\tau \propto w_\infty - w \tag{4}$$

where w is axial displacement in the fiber and w_∞ is the axial displacement for the corresponding unbroken, infinitely long fiber in an infinitely long amount of matrix. Or equivalently, as stated by Cox (1952), the axial displacement in the absence of the fiber. In mathematical terms, w_∞ is the matrix displacement at large r and w is the fiber displacement at small r which leads to

$$\tau \propto \frac{\partial w}{\partial r} \tag{5}$$

By an exact elasticity analysis, the shear stress should be given by

$$\tau = G\gamma = G\left(\frac{\partial w}{\partial r} + \frac{\partial u}{\partial z}\right) \tag{6}$$

where γ is the engineering shear strain and u is radial displacement. The Cox (1952) assumption, which will be referred to here as the fundamental shear-lag assumption, is thus that

$$\gamma = \frac{\partial w}{\partial r} \tag{7}$$

This assumption is formally exact when $\partial u/\partial z = 0$, but it should be expected to give a good approximate solution provided it can be shown that

$$\left|\frac{\partial u}{\partial z}\right| << \left|\frac{\partial w}{\partial r}\right| \tag{8}$$

Cox's (1952) original analysis has lead to wide-spread use of shear-lag models for analysis of stress transfer in composites (*e.g.*, Kim, Baillie, and Mai, 1991; Jiang and Penn, 1992; Hseuh, 1995 and references therein). In other words, the fundamental shear-lag approximation is often taken as an acceptable approximation for composite stress analysis. Here I will examine the suitability of shear-lag methods for analyzing stress transfer and energy in axisymmetric fiber/matrix problems. The approach will be to begin with exact elasticity equations for axisymmetric stress states with transversely isotropic materials and then to introduce the minimum assumptions required to arrive at Cox's (1952) equation. I am aware of two other attempts at deriving shear-lag methods directly from elasticity equations by Nayfeh (1977) and McCartney (1992). The approach here is a generalization of those papers to more explicitly state the required assumptions, to handle a wider variety of problems (*e.g.*, multiple concentric cylinders), and to consider shear-lag predictions of strain energy.

Besides Cox's (1952) fundamental shear-lag assumptions, at least three additional assumptions must be made to derive the equations typically used for shear-lag models. Furthermore, the elasticity analysis leads to a shear-lag parameter, β, that is drastically different than the $\beta_{\rm cox}$ proposed by Cox (1952). For two-cylinder problems, the β derived here agrees with the β's derived by Nayfeh (1977) and McCartney (1992). Using the improved β, shear-lag methods give reasonable estimates of both stress transfer and energy in finite, two-cylinder, fiber/matrix problems. The shear-lag method, however, does not work for low fiber volume fractions (*i.e.*, fiber in an infinite matrix), does not work well for displacement boundary conditions, and is probably too qualitative for calculations of shear stress or energy release rate.

2. Theory

2.1. Exact Elasticity Results

Consider axisymmetric stress states and let $u(r,z)$ and $w(r,z)$ be the radial and axial displacements, respectively. The hoop displacements (v) are always zero and the radial and axial displacements depend only on the radial and axial coordinates, r and z. The axial and shear strains are given in terms of displacements by

$$\varepsilon_{zz} = \frac{\partial w}{\partial z} \qquad \text{and} \qquad \gamma_{rz} = \frac{\partial u}{\partial z} + \frac{\partial w}{\partial r} \tag{9}$$

These strains are related to stresses by Hooke's laws:

$$\varepsilon_{zz} = \frac{\sigma_{zz}}{E_A} - \frac{\nu_A}{E_A}(\sigma_{rr} + \sigma_{\theta\theta}) + \alpha_A T \qquad \text{and} \qquad \gamma_{rz} = \frac{\tau_{rz}}{G_A} \tag{10}$$

The axial and shear stresses must further satisfy the axial equilibrium equation

$$\frac{\partial \tau_{rz}}{\partial r} + \frac{\partial \sigma_{zz}}{\partial z} + \frac{\tau_{rz}}{r} = 0 \tag{11}$$

For brevity, only the axisymmetric elasticity equations used in this paper are quoted. The material has been assumed to be transversely isotropic with the axial direction of the material aligned with the axial direction of the stress state. E_A and E_T are the axial and transverse tensile moduli, G_A is the axial shear modulus, and ν_T is the transverse Poisson's ratio. A thermal stress term is included to account for residual stresses; α_A is the axial thermal expansion coefficient and $T = T_s - T_0$ is the difference between the specimen temperature, T_s, and the stress-free temperature, T_0.

From Lekhnitski (1981), the stresses and displacements for an axisymmetric stress state in a transversely isotropic material can be written as (again quoting only what will be used):

$$\sigma_{zz} = \frac{\partial}{\partial z}\left(c\frac{\partial^2\Psi}{\partial r^2} + \frac{c}{r}\frac{\partial \Psi}{\partial r} + d\frac{\partial^2\Psi}{\partial z^2}\right) \tag{12}$$

$$\tau_{rz} = \frac{\partial}{\partial r}\left(\frac{\partial^2\Psi}{\partial r^2} + \frac{1}{r}\frac{\partial \Psi}{\partial r} + a\frac{\partial^2\Psi}{\partial z^2}\right) \tag{13}$$

$$u = \frac{b-1}{2G_T}\frac{\partial^2\Psi}{\partial r \partial z} \tag{14}$$

where the constants are

$$a = \frac{-\nu_A(1+\nu_T)}{1 - \frac{\nu_A^2 E_T}{E_A}} \tag{15}$$

$$b = \frac{\nu_T - \frac{\nu_A E_T}{E_A}\left(\frac{E_A}{G_A} - \nu_A\right)}{1 - \frac{\nu_A^2 E_T}{E_A}} \tag{16}$$

$$c = \frac{\frac{E_A}{G_A} - \nu_A(1+\nu_T)}{1 - \frac{\nu_A^2 E_T}{E_A}} \tag{17}$$

$$d = \frac{\frac{E_A}{2G_T}(1-\nu_T)}{1 - \frac{\nu_A^2 E_T}{E_A}} \tag{18}$$

and G_T and ν_A are the transverse shear modulus and axial Poisson's ratio. For a transversely isotropic material, the transverse tensile and shear moduli are related by $E_T = 2G_T(1+\nu_T)$. The stress function Ψ must satisfy the equation

$$\nabla_1^2\nabla_2^2\Psi = 0 \tag{19}$$

where the operators are defined by

$$\nabla_i^2 = \frac{\partial^2}{\partial r^2} + \frac{1}{r}\frac{\partial}{\partial r} + \frac{1}{s_i^2}\frac{\partial^2}{\partial z^2} \tag{20}$$

and the constants, s_1 and s_2 are

$$s_{1,2}^2 = \frac{a+c \pm \sqrt{(a+c)^2 - 4d}}{2d} \tag{21}$$

The fundamental shear-lag assumption that $\partial u/\partial z = 0$ implies that u is a function only of r. We can consider the conditions for which the fundamental shear-lag assumption will lead to an exact solution. Let $u = g_1(r)$ be a function only of r. Integrating Eq. (14) twice, the stress function must have the form

$$\Psi = f(z) + g_1(r)z + g_2(r) \tag{22}$$

where $f(z)$ is a function only of z and $g_i(r)$ are functions only of r. Substituting into Eq. (19), the differential equations for the unknown functions in terms of r, z, and a set of constants, k_i become:

$$f''(z) = -\frac{k_1 s_1^2 s_2^2 z^3}{6} - \frac{k_2 s_1^2 s_2^2 z^2}{2} + k_7 z + k_8 \tag{23}$$

$$g_1''(r) + \frac{g_1'(r)}{r} = \frac{k_1 r^2}{4} + k_3 \ln r + k_4 \tag{24}$$

$$g_2''(r) + \frac{g_2'(r)}{r} = \frac{k_2 r^2}{4} + k_5 \ln r + k_6 \tag{25}$$

Using Eqs. (12) and (13) one quickly obtains

$$\sigma_{zz} = c\left(\frac{k_1^2 r}{4} + k_3 \ln r + k_4\right) - d\left(\frac{k_1 z^2}{2d} + \frac{k_2 z}{d} - k_7\right) \tag{26}$$

$$\tau_{rz} = \frac{r}{2}(k_1 z + k_2) + \frac{1}{r}(k_3 z + k_5) \tag{27}$$

Focusing on one value of r, say the interface between a cylindrical fiber and a matrix, σ_{zz} is quadratic in z and τ_{rz} is linear in z; no other forms for σ_{zz} and τ_{rz} are possible when the fundamental shear-lag approximation is correct. With the exception of elasto-plastic models, where τ_{rz} is assumed to be constant and σ_{zz} is therefore linear, the exact solutions to stress transfer problems do not follow these simple forms for σ_{zz} and τ_{rz}. Thus, as anticipated, shear-lag methods can only provide approximate analyses for stress transfer problems. They can be expected to be good approximations in regions where τ_{rz} does not deviate too far from linearity in z; they might be a poor approximations when τ_{rz} is non-linear in z.

2.2. Approximate Shear-Lag Analysis

The fundamental shear-lag assumption by itself is not enough to derive an approximate shear-lag analysis of stress transfer; additional assumptions are required. The choices for the additional assumptions are not unique. The goal here was to select a set of additional assumptions that are consistent with the bulk of the shear-lag literature. The next key assumption is found be rewriting the form of the "exact" shear-lag shear stress in a more general form

$$\tau_{rz} = \frac{f_0(z)r}{2} + \frac{f_1(z)}{r} \tag{28}$$

where $f_i(z)$ are functions of only z. In the "exact" shear-lag stress state, $f_i(z)$ are linear in z; in an approximate shear-lag analysis we relax this requirement and let $f_i(z)$ be arbitrary functions of z (McCartney, 1992). A similar assumption or a similar form for the resulting shear stress is found in most shear-lag papers in the literature.

Now consider a hollow cylinder of a transversely isotropic material with the inner radius r_i and the outer radius r_o. Let

$$\tau_{rz}(r_i) = \tau_{rz}(r_i, z) \qquad \text{and} \qquad \tau_{rz}(r_o) = \tau_{rz}(r_o, z) \tag{29}$$

be the inner and outer surface shear stresses. These surface stresses are functions only of z. The functions $f_i(z)$ can be expressed in terms of $\tau_{rz}(r_i)$ and $\tau_{rz}(r_o)$. The form of the shear stresses becomes:

$$\tau_{rz} = \frac{r_i r_o}{(r_o^2 - r_i^2)}\left[\tau_{rz}(r_i)\left(\frac{r_o}{r} - \frac{r}{r_o}\right) - \tau_{rz}(r_o)\left(\frac{r_i}{r} - \frac{r}{r_i}\right)\right] \tag{30}$$

The next step is to generalize a transform technique used by McCartney (1992) — equate τ_{rz} in Eq. (30) to $G_A \frac{\partial w}{\partial r}$, multiply both sides by $(A - r^2)$, where A is a constant, and integrate by parts from r_i to r_o to get

$$\begin{aligned} \langle w \rangle (r_o^2 - r_i^2) \quad = \quad & \frac{r_i \tau_{rz}(r_i)}{2G_A} r_i \tau_{rz}(r_i) \left(\frac{A r_o^2}{r_o^2 - r_i^2} \ln \frac{r_o^2}{r_i^2} - A - r_o^2 + \frac{r_o^2 + r_i^2}{2}\right) + w(r_i)(A - r_i^2) \\ & - \frac{r_o \tau_{rz}(r_o)}{2G_A}\left(\frac{A r_i^2}{r_o^2 - r_i^2} \ln \frac{r_o^2}{r_i^2} - A - r_i^2 + \frac{r_o^2 + r_i^2}{2}\right) - w(r_o)(A - r_o^2) \end{aligned} \tag{31}$$

where $\langle w \rangle$ is the average value of w defined by

$$\langle w \rangle = \frac{2}{r_o^2 - r_i^2} \int_{r_i}^{r_o} r w \, dr \tag{32}$$

and $w(r_i)$ and $w(r_o)$ are the surface displacements. $\langle w \rangle$, $w(r_i)$, and $w(r_o)$ are all functions of only z.

To deal with $\langle w \rangle$, consider an averaged form of the axial Hooke's law:

$$\langle \varepsilon_{zz} \rangle = \frac{\partial \langle w \rangle}{\partial z} = \frac{\langle \sigma_{zz} \rangle}{E_A} - \frac{\nu_A}{E_A} \langle \sigma_{rr} + \sigma_{\theta\theta} \rangle + \alpha_A T \tag{33}$$

where $\langle f \rangle$ denotes averaging over the cylinder as in Eq. (32). There is a problem — what can be assumed about $\langle \sigma_{rr} + \sigma_{\theta\theta} \rangle$. An assumption used in virtually all shear-lag analyses is to replace the correct axial Hooke's law with a one-dimensional version that ignores transverse stresses (*e.g.*, Cox, 1952; Hseuh, 1988). The implied, though normally unstated, assumption is that

$$\langle \sigma_{rr} + \sigma_{\theta\theta} \rangle = 0 \tag{34}$$

or more explicitly that

$$\left|\frac{\nu_A}{E_A} \langle \sigma_{rr} + \sigma_{\theta\theta} \rangle\right| << \left|\frac{\langle \sigma_{zz} \rangle}{E_A} + \alpha_A T\right| \tag{35}$$

Using this new assumption and differentiating with respect to z gives

$$\frac{\partial^2 \langle w \rangle}{\partial z^2} = \frac{1}{E_A} \frac{\partial \langle \sigma_{zz} \rangle}{\partial z} = \frac{2}{E_A(r_o^2 - r_i^2)} \left[r_i \tau_{rz}(r_i) - r_o \tau_{rz}(r_o)\right] \tag{36}$$

The latter part of Eq. (36) follows by integrating the axial equilibrium equation (Eq. (11)). Finally, differentiating Eq. (31) twice and equating to Eq. (36) with $A = r_i^2$ or $A = r_o^2$ gives

$$\begin{aligned} w''(r_o) \quad = \quad & \frac{2}{E_A(r_o^2 - r_i^2)} \left[r_i \tau_{rz}(r_i) - r_o \tau_{rz}(r_o)\right] - \frac{r_i^2}{2G_A(r_o^2 - r_i^2)} \left[r_i \tau''_{rz}(r_i) \left(\frac{r_o^2}{r_o^2 - r_i^2} \ln \frac{r_o^2}{r_i^2} - 1 - \frac{r_o^2 - r_i^2}{2r_i^2}\right)\right. \\ & \left. - r_o \tau''_{rz}(r_o) \left(\frac{r_i^2}{r_o^2 - r_i^2} \ln \frac{r_o^2}{r_i^2} - 1 + \frac{r_o^2 - r_i^2}{2r_i^2}\right)\right] \end{aligned} \tag{37}$$

$$\begin{aligned} w''(r_i) \quad = \quad & \frac{2}{E_A(r_o^2 - r_i^2)} \left[r_i \tau_{rz}(r_i) - r_o \tau_{rz}(r_o)\right] - \frac{r_o^2}{2G_A(r_o^2 - r_i^2)} \left[r_i \tau''_{rz}(r_i) \left(\frac{r_o^2}{r_o^2 - r_i^2} \ln \frac{r_o^2}{r_i^2} - 1 - \frac{r_o^2 - r_i^2}{2r_o^2}\right)\right. \\ & \left. - r_o \tau''_{rz}(r_o) \left(\frac{r_i^2}{r_o^2 - r_i^2} \ln \frac{r_o^2}{r_i^2} - 1 + \frac{r_o^2 - r_i^2}{2r_o^2}\right)\right] \end{aligned} \tag{38}$$

These two equations are the most fundamental starting equations for shear-lag analysis of axisymmetric stress states. There are two equations and four unknown functions of z — $w(r_i)$, $w(r_o)$, $\tau_{rz}(r_i)$, and $\tau_{rz}(r_o)$. The two equations can be solved for two of the unknown functions. When shear-lag analysis is used for composite problems, the two remaining unknown functions will follow by boundary conditions or by continuity with the stresses and displacements with a neighboring cylinder typically having different material properties.

Once $\tau_{rz}(r_i)$ and $\tau_{rz}(r_o)$ are known, the shear stress is known every place by substitution into Eq. (30). Integrating the shear-strain Hooke's law in Eq. (10) and using $\partial u/\partial z = 0$, the axial displacement is known every place by

$$w = w(r_i) + \frac{r_i r_o}{2G_A(r_o^2 - r_i^2)}\left[r_o\tau_{rz}(r_i)\left(\ln\frac{r^2}{r_i^2} - \frac{r^2 - r_i^2}{r_o^2}\right) - r_i\tau_{rz}(r_o)\left(\ln\frac{r^2}{r_i^2} - \frac{r^2 - r_i^2}{r_i^2}\right)\right] \tag{39}$$

Integrating Eq. (11), the axial stress is

$$\sigma_{zz} = \frac{2}{r_o^2 - r_i^2}\left[r_i\int\tau_{rz}(r_i)dz - r_o\int\tau_{rz}(r_o)dz\right] + g_0(r) \tag{40}$$

The axial stress is determined except for an unknown function of r. Most shear-lag papers either assume σ_{zz} is independent of r, in which case $g_0(r)$ is a constant, or more generally deal only with the average axial stress

$$\langle\sigma_{zz}\rangle = \frac{2}{r_o^2 - r_i^2}\left[r_i\int\tau_{rz}(r_i)dz - r_o\int\tau_{rz}(r_o)dz\right] + \langle g_0(r)\rangle \tag{41}$$

where $\langle g_0(r)\rangle$ is a constant. In many problems $\langle g_0(r)\rangle$ can be determined from the boundary conditions, but in some problems it may remain undetermined. Using the assumption that $\langle\sigma_{rr} + \sigma_{\theta\theta}\rangle = 0$ and the relation for transverse stress equilibrium, it is possible to derive the form of the transverse normal stresses. It is unlikely, however, that the information buried this deep in the approximate shear-lag analysis will be accurate. Shear-lag is thus best treated as a one-dimensional analysis method that is aimed at deriving σ_{zz} and τ_{rz}, but is not suited for finding accurate information about transverse normal stresses.

The axial and shear stresses satisfy the axial equilibrium equation (Eq. (11)) and the axial displacement satisfies the shear-strain Hooke's law (Eq. (10) with $\frac{\partial u}{\partial z} = 0$). The axial displacement, does not satisfy the axial strain Hooke's law (Eq. (10)), but the *average* axial displacement does satisfy the *average* axial strain Hooke's law (Eq. (33)). There is thus a final shear-lag assumption — σ_{zz} and w should be independent of r. Because they, in general, will not be independent of r (see Eq. (39) and Eq. (40)), the final shear-lag approximation is that σ_{zz} and w should only weakly depend on r.

In summary, derivation of the most basic shear-lag equations requires using four assumptions. The four assumptions are:

$$\left|\frac{\partial u}{\partial z}\right| << \left|\frac{\partial w}{\partial r}\right| \tag{42}$$

$$\tau_{rz} = \frac{f_0(z)r}{2} + \frac{f_1(z)}{r} \tag{43}$$

$$\left|\frac{\nu_A}{E_A}\langle\sigma_{rr} + \sigma_{\theta\theta}\rangle\right| << \left|\frac{\langle\sigma_{zz}\rangle}{E_A} + \alpha_A T\right| \tag{44}$$

and that σ_{zz} and w only weakly depend on r. These assumptions appear to be the minimum number of assumptions required, but they are not a unique set of assumptions. This set was selected to be consistent with as much of the literature as possible. The use of different assumptions may be appropriate for certain problems. For example, Nayfeh (1977) considered shear-lag analysis of two concentric cylinders where the transverse strain was assumed to be small instead of the sum of the transverse stresses. He derived equations identical to those discussed in the next section, but his equations had modified coefficients. In other words, the use of altered assumptions will not alter the fundamental form of the shear-lag equations and therefore will not alter this assessment of the applicability of shear-lag methods to composite stress analysis.

3. Analysis of Concentric Cylinders

3.1. Multiple Concentric Cylinders

Consider n concentric cylinders under total axial stress of σ_0. Cylinder i extends from r_{i-1} to r_i. The shear stress on the inner surface of the first cylinder (which may be at $r_0 = 0$) is zero ($\tau_{rz}(r_0) = 0$). The shear stress on the outer surface of the last cylinder is zero ($\tau_{rz}(r_n) = 0$). The axial and shear moduli in cylinder i are $E_A^{(i)}$ and $G_A^{(i)}$.

A set of $n-1$ equations for the $n-1$ interfacial shear stresses between the n cylinders follows directly from Eq. (38). The procedure is to equate $w''(r_i)$ determined from the outer surface of cylinder i to $w''(r_i)$ determined from the inner surface of cylinder $i+1$. The result is:

$$\begin{aligned}
2\left[\frac{r_{i-1}\tau_{rz}(r_{i-1})}{E_A^{(i)}(r_i^2-r_{i-1}^2)} - r_i\tau_{rz}(r_i)\left(\frac{1}{E_A^{(i)}(r_i^2-r_{i-1}^2)} + \frac{1}{E_A^{(i+1)}(r_{i+1}^2-r_i^2)}\right) + \frac{r_{i+1}\tau_{rz}(r_{i+1})}{E_A^{(i+1)}(r_{i+1}^2-r_i^2)}\right] = \\
+ \frac{r_{i-1}^3\tau''_{rz}(r_{i-1})}{2G_A^{(i)}(r_i^2-r_{i-1}^2)}\left(\frac{r_i^2}{r_i^2-r_{i-1}^2}\ln\frac{r_i^2}{r_{i-1}^2} - 1 + \frac{r_i^2-r_{i-1}^2}{2r_{i-1}^2}\right) \\
- r_i\tau''_{rz}(r_i)\left[\frac{r_{i-1}^2}{2G_A^{(i)}(r_i^2-r_{i-1}^2)}\left(\frac{r_{i-1}^2}{r_i^2-r_{i-1}^2}\ln\frac{r_i^2}{r_{i-1}^2} - 1 + \frac{r_i^2-r_{i-1}^2}{2r_{i-1}^2}\right)\right. \\
\left. + \frac{r_{i+1}^2}{2G_A^{(i+1)}(r_{i+1}^2-r_i^2)}\left(\frac{r_{i+1}^2}{r_{i+1}^2-r_i^2}\ln\frac{r_{i+1}^2}{r_i^2} - 1 - \frac{r_{i+1}^2-r_i^2}{2r_{i+1}^2}\right)\right] \\
+ \frac{r_{i+1}^3\tau''_{rz}(r_{i+1})}{2G_A^{(i+1)}(r_{i+1}^2-r_i^2)}\left(\frac{r_i^2}{r_{i+1}^2-r_i^2}\ln\frac{r_{i+1}^2}{r_i^2} - 1 + \frac{r_{i+1}^2-r_i^2}{2r_{i+1}^2}\right)
\end{aligned} \tag{45}$$

The set of equations for $i = 1$ to $n-1$ define $n-1$ coupled, second-order differential equations for the $n-1$ interfacial shear stresses. Once the interfacial shear stresses are found, the shear stress, axial displacement, and average axial stress (to within a constant) follow from the results in the previous section. This analysis assumed continuous displacements between cylinders and thus assumes perfect interfaces between all cylinders. Imperfect interfaces could, in principle, be modeled by allowing displacement discontinuities at some interfaces (Hashin, 1990); only perfect interfaces are considered here.

3.2. Two Concentric Cylinders

A common problem analyzed by shear-lag methods is a solid fiber cylinder of radius r_1 embedded in a hollow matrix cylinder with inner radius r_1 and outer radius r_2. A special case of the previous section (using $n = 2$ and $r_0 = 0$) gives the single equation

$$\frac{\partial^2\tau_{rz}(r_1)}{\partial z^2} - \beta^2\tau_{rz}(r_1) = 0 \tag{46}$$

where

$$\beta^2 = \frac{2}{r_1^2E_A^{(1)}E_A^{(2)}}\left[\frac{E_A^{(1)}V_1 + E_A^{(2)}V_2}{\frac{V_2}{4G_A^{(1)}} + \frac{1}{2G_A^{(2)}}\left(\frac{1}{V_2}\ln\frac{1}{V_1} - 1 - \frac{V_2}{2}\right)}\right] \tag{47}$$

and V_1 and V_2 are the fiber and matrix volume fractions defined by

$$V_1 = \frac{r_1^2}{r_2^2} \qquad \text{and} \qquad V_2 = \frac{r_2^2 - r_1^2}{r_2^2} \tag{48}$$

Multiplying the axial equilibrium equation in the fiber by r and integrating from 0 to r_1 gives

$$\frac{\partial\langle\sigma_f\rangle}{\partial z} = -\frac{2\tau_{rz}(r_1)}{r_1} \tag{49}$$

where σ_f is σ_{zz} in the fiber (see Eq. (3) or Eq. (36)). Substitution into Eq. (46) and integrating once gives

$$\frac{\partial^2 \langle \sigma_f \rangle}{\partial z^2} - \beta^2 \langle \sigma_f \rangle = constant \tag{50}$$

Now, far away from stress transfer zone, the fiber axial stress will settle into the far-field stress, $\sigma_{f\infty}$, and the derivative term will be zero. The *constant* must therefore be $-\beta^2 \langle \sigma_{f\infty} \rangle$. The final equation, which is identical to Cox's (1952) equation is

$$\frac{\partial^2 \langle \sigma_f \rangle}{\partial z^2} - \beta^2 \langle \sigma_f \rangle = -\beta^2 \langle \sigma_{f\infty} \rangle \tag{51}$$

The β^2 term (Eq. (47)), however, is very different than the one derived by Cox (1952) (Eq. (2)). The β^2 term here is identical to the one derived by Nayfeh (1977) and McCartney (1992).

3.3. *A Specific Problem*

Consider concentric fiber and matrix cylinders of length l with a total applied axial stress of σ_0. The fiber ends are treated as fiber breaks and therefore the fiber-end surfaces are stress free. The entire applied axial stress is assumed to be applied uniformly over the matrix at a stress level of

$$\sigma_m = \frac{\sigma_0}{V_2} \tag{52}$$

All boundary shear stresses are zero. For simplicity, thermal stresses are ignored or $T = 0$. Equation (51) along with Hooke's laws, force balance, and equilibrium are easily solved to give

$$\frac{\langle \sigma_f \rangle}{\langle \sigma_{f\infty} \rangle} = 1 - \frac{\cosh \beta z}{\cosh \frac{\beta l}{2}} \tag{53}$$

$$\frac{\tau_f}{\langle \sigma_{f\infty} \rangle} = \frac{r\beta}{2} \frac{\sinh \beta z}{\cosh \frac{\beta l}{2}} \tag{54}$$

$$\frac{\langle w_f \rangle}{\langle \sigma_{f\infty} \rangle} = \frac{1}{E_A^{(1)}} \left(z - \frac{\sinh \beta z}{\beta \cosh \frac{\beta l}{2}} \right) \tag{55}$$

$$\frac{\langle \sigma_m \rangle}{\langle \sigma_{f\infty} \rangle} = \frac{\sigma_{m\infty}}{\sigma_{f\infty}} + \frac{V_1}{V_2} \frac{\cosh \beta z}{\cosh \frac{\beta l}{2}} \tag{56}$$

$$\frac{\tau_m}{\langle \sigma_{f\infty} \rangle} = \frac{V_1 \beta}{2V_2} \frac{\sinh \beta z}{\cosh \frac{\beta l}{2}} \left(\frac{r_2^2}{r} - r \right) \tag{57}$$

$$\frac{\langle w_m \rangle}{\langle \sigma_{f\infty} \rangle} = \frac{1}{E_A^{(2)}} \left(\frac{\sigma_{m\infty}}{\sigma_{f\infty}} z + \frac{V_1}{V_2} \frac{\sinh \beta z}{\beta \cosh \frac{\beta l}{2}} \right) \tag{58}$$

where τ_f is τ_{rz} in the fiber, w_f is w in the matrix, σ_m is σ_{zz} in the matrix, $\sigma_{m\infty}$ is the far-field σ_{zz} in the matrix, τ_m is τ_{rz} in the matrix, and w_m is w in the matrix. The origin for the z axis was placed in the middle of the fiber which places the fiber ends or breaks at $z = \pm l/2$. The interfacial shear stress, which is continuous from the fiber to the matrix, is

$$\frac{\tau_{rz}(r_1)}{\langle \sigma_{f\infty} \rangle} = \frac{r_1 \beta}{2} \frac{\sinh \beta z}{\cosh \frac{\beta l}{2}} \tag{59}$$

A complementary problem is when the entire axial load is carried by the fiber and the matrix ends have zero stress. The fiber axial stress boundary condition is

$$\sigma_f = \frac{\sigma_0}{V_1} \tag{60}$$

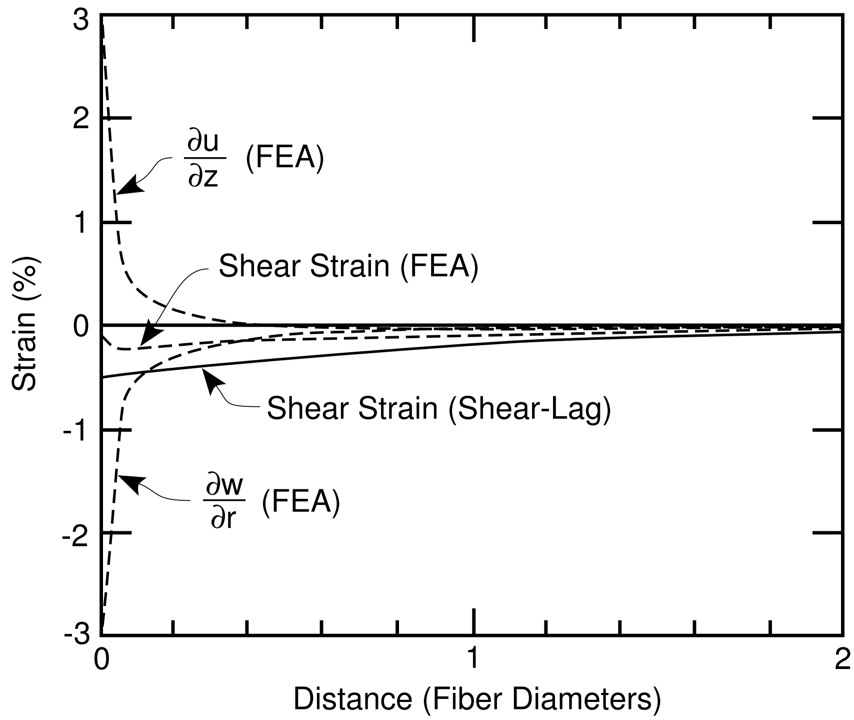

Fig. 1. A plot of $\frac{\partial u}{\partial z}$, $\frac{\partial w}{\partial r}$, and γ_{rz} all evaluated by finite element analysis (dashed lines) compared to γ_{rz} evaluated by shear-lag analysis (solid line). The results are plotted along the fiber matrix interface as a function of distance (in fiber diameters) from the fiber break. All terms are plotted in percent strain. The modulus ratio was $E_f/E_m = 10$, the fiber volume fraction was $V_1 = 10\%$, and the total axial stress was adjusted to make $\sigma_{f\infty} = 100$ MPa.

This problem is appropriate, for example, for analysis of the fiber-pull out test (Jiang and Penn, 1992). The solution to the pull-out problem can be recovered from the above fiber break problem by superposition with the far-field stresses. For example, the average axial fiber stress in the pull-out analysis is

$$\frac{\langle\sigma_f\rangle}{\langle\sigma_{f\infty}\rangle} = 1 + \frac{\langle\sigma_{m\infty}\rangle\, V_2}{\langle\sigma_{f\infty}\rangle\, V_1}\frac{\cosh\beta z}{\cosh\frac{\beta l}{2}} \tag{61}$$

The stress transfer term is identical to the stress transfer term in the fiber break problem. Thus any conclusions drawn about stress transfer analysis of the fiber break problem apply also to stress transfer in the pull-out problem. The next section considers only the fiber break problem.

4. Results

This section describes a set of analyses for an isotropic fiber of radius 0.5 mm and length 10 mm embedded in an isotropic matrix. The matrix properties were taken to be $E_A^{(2)} = 2500$ MPa and $\nu_A^{(2)} = 0.333$. The fiber properties were taken to be $E_A^{(1)} = 2500(E_f/E_m)$ and $\nu_A^{(1)} = 0.25$. Because the materials are isotropic, the shear moduli are

$$G_A^{(2)} = 937 \text{ MPa} \qquad \text{and} \qquad G_A^{(1)} = 937\frac{E_f}{E_m} \tag{62}$$

The fiber/matrix modulus ratio, E_f/E_m, and the fiber volume fraction, V_1 were varied. Because of the selected fiber radius, the distance units can be interpreted as distances in units of fiber diameters and the fiber fragment has an aspect ratio of 10. The validity of the shear-lag assumptions and the accuracy of the shear-lag results were evaluated by comparing shear-lag predictions to finite element analysis (FEA).

The FEA software was modified to plot $\frac{\partial u}{\partial z}$ and $\frac{\partial w}{\partial r}$ rather than plotting only their sum or the shear strain, γ_{rz}. This modification was used to evaluate the fundamental shear-lag assumption that $\frac{\partial u}{\partial z} << \frac{\partial w}{\partial r}$.

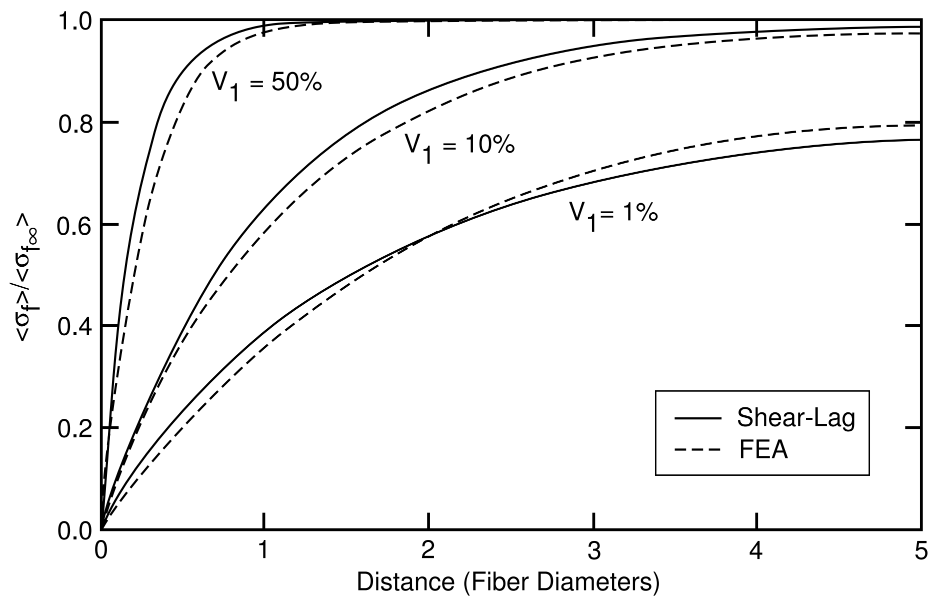

Fig. 2. A plot of $\langle\sigma_f\rangle$ / $\langle sfi\rangle$ evaluated by finite element analysis (dashed lines) and by shear-lag analysis (solid lines). The results are for the modulus ratio $E_f/E_m = 10$ and various fiber volume fractions (V_1).

The results at the fibre/matrix interface as a function of distance from the fiber break when $E_f/E_m = 10$ and $V_1 = 10\%$ are given in Fig. 1. For these conditions, the bulk of the stress transfer occurs within the first two fiber diameters from the fiber break. Over the entire stress transfer zone, the fundamental shear-lag approximation is never valid. In fact $\frac{\partial u}{\partial z}$ and $\frac{\partial w}{\partial r}$ are similar in magnitude, although opposite in sign. They combine to give a much smaller shear-strain. Despite the problems with the fundamental shear-lag approximation, the shear-lag shear strain is much closer to the FEA shear strain than it is to $\frac{\partial w}{\partial r}$. The magnitude of the shear-lag shear strain, however, is too high by more than a factor of two. Furthermore, the shear-lag shear strain peaks at the fiber break while the correct solution, as approximately seen in the FEA solution, should be zero to satisfy the fiber surface stress-free boundary conditions.

The FEA software was further modified to plot average stresses. Figure 2 plots the average fiber stress as a function of distance from the fiber break when $E_f/E_m = 10$ and for volume fractions of $V_1 = 50\%$, 10%, and 1%. Considering the problems with the fundamental shear-lag approximation, shear-lag analysis does a surprising good job of predicting average axial stress in the fiber. The shear-lag equations always lead to an exponential form for the stresses (or hyperbolic functions for finite length fibers). The observation that the shear-lag predictions cross over the FEA calculations (see $V_1 = 1\%$ in Fig. 2) show that stress transfer is not precisely exponential.

To better judge the overall accuracy of shear-lag analysis, we defined a 50% transfer length, z_{50}, as the number of fiber diameters required for $\langle\sigma_f\rangle$ to reach 50% of the far-field stress, $\langle\sigma_{f\infty}\rangle$. By a shear-lag analysis

$$z_{50} = \frac{1}{\beta}\cosh^{-1}\left(\frac{1}{2}\cosh\frac{\beta l}{2}\right) \tag{63}$$

The shear-lag results are compared to FEA results in Fig. 3 for modulus ratios of $E_f/E_m = 100$, 10, or 1 and for volume fractions over the range from $V_1 = 0$ to 70%. A fiber volume fraction of $V_1 = 0$ corresponds to a fiber in an infinite matrix. Overall, shear-lag does a good *qualitative* job of predicting stress transfer. The emphasis was intentionally placed on "qualitative." While shear-lag predicts all the trends of stress transfer, the absolute transfer rate is off by 10-20% for modulus ratios of 100 and 10 and off by up to 50% for a modulus ratio of 1. It is interesting that at low fiber volume fraction, stress transfer gets slower as the modulus ratio gets higher, but at high fiber volume fractions the reverse is true. There also appears to be an "iso-transfer" fiber volume fraction where the stress transfer rate is independent of modulus ratio. Shear-lag correctly predicts all trends in transfer rate with changing modulus ratio of fiber volume fraction,

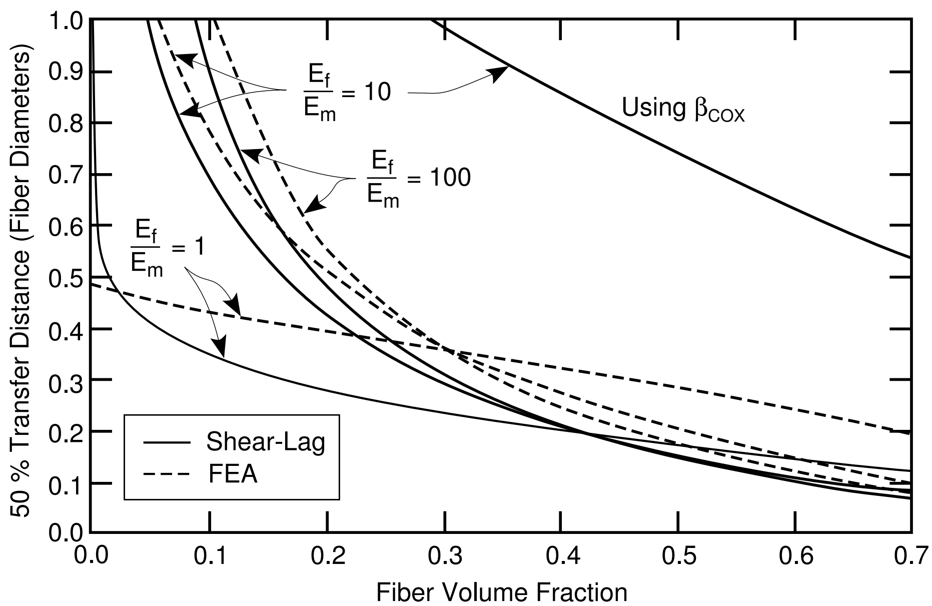

Fig. 3. The 50% stress transfer distance (in fiber diameters) as a function of the fiber volume fraction for various modulus ratios. For each modulus ratio there are plots for shear-lag analysis (solid lines) and for FEA analysis (dashed lines). The curve in the upper-right hand corner are the 50% stress transfer rate predictions using a shear-lag analysis with the shear-lag parameter recommended by Cox (1952) (β_{cox}).

but it predicts the iso-transfer volume fraction to be at $V_1 = 42\%$ while the correct result (as calculated by FEA analysis) is at $V_1 = 31\%$.

The curve in the upper-right hand corner of Fig. 3 is the shear-lag prediction of stress transfer for $E_f/E_m = 10$ assuming the shear-lag parameter is given by the Cox (1952) result (β_{cox} in Eq. (2)) with $s = r_2$ instead of the shear-lag parameter derived here (β in Eq. (47)). The Cox (1952) shear-lag parameter, β_{cox}, is grossly in error; it should be abandoned in all shear-lag analyses of composites. A literal interpretation of Cox's (1952) analysis uses $s = 2r_2$. Because

$$\ln\frac{r_2}{r_1} = \frac{1}{2}\ln\frac{1}{V_1} \qquad \text{and} \qquad \ln\frac{2r_2}{r_1} = \frac{1}{2}\ln\frac{4}{V_1} \tag{64}$$

the use of $s = 2r_2$ effectively scales the volume fraction axis (the x axis) by a factor of four. This expansion causes the β_{cox} predictions shift to the right and be even further in error than when using β_{cox} with $s = r_2$.

Shear-lag analysis has serious limitations when considering very low fiber volume fractions, or equivalently when considering analysis for a fiber in an infinite matrix. Taking the limit as $V_1 \to 0$ gives

$$\lim_{V_1\to 0}\beta = \lim_{V_1\to 0}\beta_{\text{cox}} = 0 \tag{65}$$

which implies, from Eq. (63), that the stress transfer length becomes infinite. In a correct analysis, the stress transfer rate should become independent of V_1 for low fiber volume fractions and become equal to the stress transfer rate for a fiber in an infinite matrix. Figure 4 plots the shear-lag and FEA stress transfer rates for a modulus ratio of $E_f/E_m = 10$ and for low fiber volume fractions. The shear-lag analyses asymptotically approach an infinite transfer distance as $V_1 \to 0$. In contrast, the FEA analysis levels off at an asymptotic transfer distance of about 1.8 fiber diameters. Clearly, shear-lag analysis breaks down for low fiber volume fractions, or, in other words, shear-lag analysis gives no information about stress transfer from a fiber into an infinite amount of matrix.

Shear-lag analysis in composites is often used to interpret results from single-fiber tests in which the specimen is a single fiber embedded in a large amount of matrix. Because such specimens can be approximated by analysis of a fiber in an infinite amount of matrix, shear-lag analysis should not be expected to provide any information about stress transfer. The only acceptable use of shear-lag analysis on such

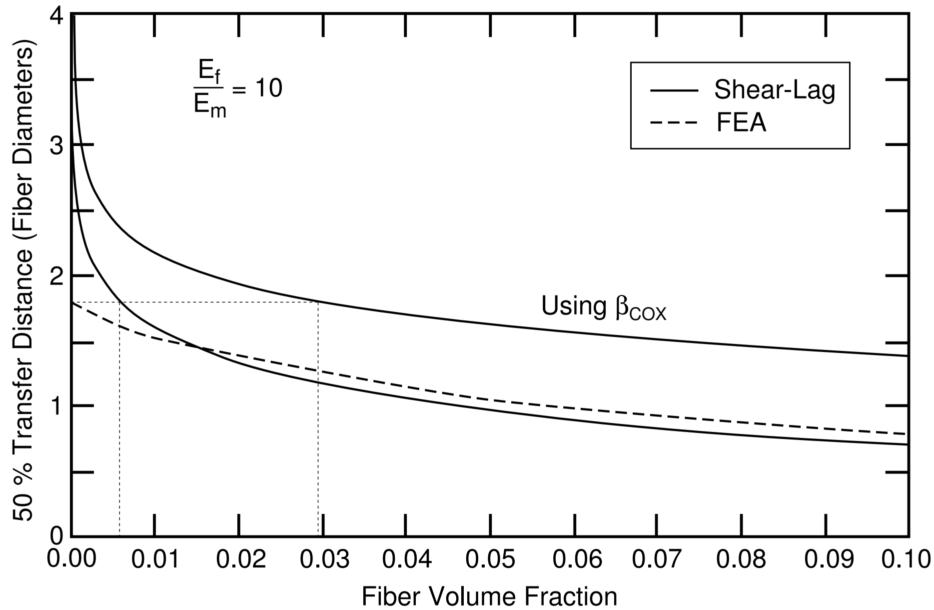

Fig. 4. The 50% stress transfer distance (in fiber diameters) as a function of the fiber volume fraction for a modulus ratio of $E_f/E_m = 10$. The two shear-lag plots (solid lines) are for the shear-lag parameter derived here (β) or for the shear-lag parameter recommended by Cox (1952) ($\beta_{\rm cox}$). The FEA calculations are given by the dashed line.

specimens is to treat β as an adjustable parameter instead of a defined constant. Indeed, many researchers have adopted just such an approach by defining an *effective* stress concentration cylinder in the matrix (Lacroix, Tilmans, Keunings, Desaeger, and Verpoest, 1992; Feillard, Désermot, and Favre, 1994; Wagner, Nairn, and Detassis, 1995). Stress transfer is determined by the fiber volume fraction within the effective cylinder rather than within the entire matrix. Figure 4 illustrates a graphical procedure for finding the effective fiber volume fraction for shear-lag analysis of a fiber in an infinite matrix. Using β in Eq. (47) the effective fiber volume fraction for $E_f/E_m = 10$ is about 0.6% which translates to an effective stress concentration cylinder radius of $r_2/r_1 = 12.9$. When using effective volume fractions, it is even permissible, as many researchers have done, to use the Cox (1952) shear-lag parameter ($\beta_{\rm cox}$). From Fig. 4 the effective fiber volume fraction when using $\beta_{\rm cox}$ for $E_f/E_m = 10$ is about 3% which translates to an effective stress concentration cylinder radius of $r_2/r_1 = 5.8$. The effective fiber volume fraction is a function of the modulus ratio, but the result calculated here using $\beta_{\rm cox}$ is similar to typical assumptions made in the literature also based on $\beta_{\rm cox}$ (Wagner, Nairn, and Detassis, 1995). Although it is formally acceptable to calculate effective fiber volume fractions by using Cox's (1952) shear-lag parameter ($\beta_{\rm cox}$), there is little incentive to do so because there is never a situation in which $\beta_{\rm cox}$ gives a correct prediction of stress transfer. Thus, even for a fiber in an infinite matrix, the Cox (1952) parameter should be abandoned in favor of defining effective stress concentration cylinders using β in Eq. (47).

Recent work on fiber breakage and interface effects has used energy methods or fracture mechanics instead of stress failure criteria (Wagner, Nairn, and Detassis, 1995; Nairn and Liu, 1996). Energy analyses can be developed using shear-lag equations, but, how accurate are shear-lag predictions for energy? Consider again the fiber break problem for a fiber in a finite amount of matrix. The entire surface of this specimen is stress free except for the uniform stress of σ_0/V_2 applied to the matrix ends. The total strain energy can thus be found most easily by integrating the surface tractions and displacements. Integrating surface work over the top and bottom matrix surfaces gives

$$U = 2 \times \frac{1}{2}\int_{r_1}^{r_2} 2\pi r \frac{\sigma_0}{V_2} w_m(r, l/2)dr = \pi r_2^2 \sigma_0 \left\langle w_m(l/2) \right\rangle \tag{66}$$

where $\langle w_m(l/2)\rangle$ is the average axial displacement on the ends of the matrix. Equation (66) is an exact expression for strain energy in the fiber-break specimen provided an exact result for $\langle w_m(l/2)\rangle$ is known.

Shear-lag analysis can be used to derive an approximate strain energy by substituting the shear result for $\langle w_m(l/2)\rangle$ given by Eq. (58). The result is

$$\frac{U}{U_\infty} = 1 + \frac{E_A^{(1)}V_1}{E_A^{(2)}V_2}\frac{\tanh\frac{\beta l}{2}}{\frac{\beta l}{2}} \tag{67}$$

where U_∞ is the energy in the absence of the fiber breaks or the energy when both the fiber and matrix stresses equal their far-field stresses:

$$U_\infty = \pi r_2^2 l \frac{\sigma_0^2}{2E_c} \tag{68}$$

Here $E_c = E_A^{(1)}V_1 + E_A^{(2)}V_2$ is the rule-of-mixtures axial modulus of the composite specimen. In deriving Eq. (67), it was assumed than

$$\sigma_{m\infty} = \frac{E_A^{(2)}}{E_c}\sigma_0 \qquad \text{and} \qquad \sigma_{m\infty} = \frac{E_A^{(1)}}{E_c}\sigma_0 \tag{69}$$

The above assumptions for E_c, $\sigma_{m\infty}$, and $\sigma_{f\infty}$ are not exact for two concentric cylinders with different Poisson ratios, but they are in error from the exact concentric cylinder results (Christenson, 1979) by less than 1%. These assumptions, thus will have no effect on the assessment of the accuracy of shear-lag analysis for predicting energy.

A comparison for shear-lag predictions of total energy to FEA calculations of total energy for $E_f/E_m =$ 100, 10, and 1 and for fiber volume fractions from 0 to 70% is given in Fig. 5. To better compare results in a single plot, Fig. 5 plots the relative change in energy, $\Delta U/U_\infty$, and normalizes each plot by the modulus ratio. The plot is thus for

$$\frac{E_m}{E_f}\frac{\Delta U}{U_\infty} = \frac{E_m}{E_f}\left(\frac{U - U_\infty}{U_\infty}\right) \tag{70}$$

Like average axial fiber stress, shear-lag analysis does a good *qualitative* job of predicting total strain energy. Shear-lag predictions for ΔU are within 10% of FEA calculations for $E_f/E_m = 100$. The errors in ΔU get larger as E_f/E_m gets smaller, but the shear-lag predictions for ΔU are always within 20% of the FEA calculations.

An alternative fiber break problem is to replace the uniform stress over the matrix end surfaces by a boundary condition of uniform displacements. A fixed-displacement boundary condition is more appropriate for analysis of the fragmentation test (Nairn, 1996). In the fragmentation test, a single fiber embedded in a matrix develops multiple, roughly periodic fiber breaks when subjected to axial stress (Wadsworth and Spilling, 1968). The analysis of individual fiber fragments from such a specimen requires the use of uniform end displacements to maintain continuity in displacements from one fiber fragment to the next (Nairn, 1996). Formally, the shear-lag analysis developed here cannot solve the constant displacement boundary condition, because the axial displacement depends on the radial coordinate. This radial dependence is evident in Eq. (39). Nevertheless, many authors have used shear-lag analysis on the fragmentation specimen (Lacroix, Tilmans, Keunings, Desaeger, and Verpoest, 1992; Feillard, Désermot, and Favre, 1994). The inconsistency can be resolved by dealing only with *average* axial displacements (*e.g.*, Eq. (58)) and average fiber and matrix stresses. By this approach, the shear-lag analysis for constant stress and constant displacement boundary conditions are identical. Thus Eqs. (53)–(58) are also the shear-lag predictions for stress transfer when the matrix end displacement is given by a constant value of w_m, provided that the far-field fiber stress is correctly calculated from applied fixed displacement.

The FEA analysis under fixed displacement conditions is more complicated than under uniform stress conditions. First, there are numerical difficulties at the fiber/matrix interface where the interface intersects the free surface. These numerical difficulties make the local calculation of interfacial stresses unreliable. Here, only the *average* fiber stress is considered and that stress is mostly considered away from the fiber break (*i.e.*, the stress transfer profile). The numerical difficulties should not strongly influence these stress transfer predictions. Second, it is not possible to *a priori* select a fixed end displacement to give a convenient far-field fiber stress of 100 MPa. The end displacement required to give a desired far-field fiber stress can only be determined after solving the problem. The FEA analysis proceeded as follows. First, an arbitrary fixed end-displacement was selected. Then, from the FEA solution the average stress over the entire specimen

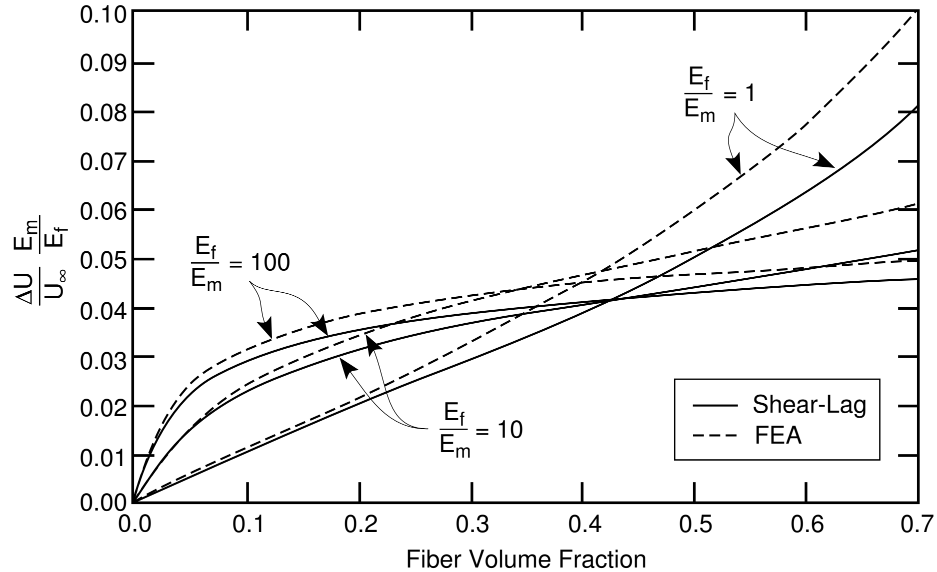

Fig. 5. Relative change in total strain energy as a function of fiber volume fraction for various values of the modulus ratio, E_f/E_m. All results have been normalized by dividing by E_f/E_m. FEA calculations are shown in dashed lines; shear-lag predictions are shown in solid lines.

was evaluated as a function of distance from the fiber break. This average stress quickly converged to a constant value which is the *effective* σ_0 for the given end displacement. Next, the *effective* σ_0 was input into a concentric cylinder analysis (Christenson, 1979) to calculate $\sigma_{f\infty}$. Finally, the evaluated $\sigma_{f\infty}$ was used to renormalize the FEA results to give an analysis with a far-field fiber stress of 100 MPa.

The average axial stress in the fiber as a function of distance from the fiber break for $E_f/E_m = 10$ and $V_1 = 10\%$ is plotted in Fig. 6. The FEA results for uniform stress and uniform displacement boundary conditions are different; the stress transfer is more rapid under fixed displacement boundary conditions than it is under uniform stress boundary conditions. Physically this effect can be explained by considering the average displacement on the fiber ends. If the matrix end displacement is plotted under uniform matrix stress conditions, it can be observed that the fiber end retracts from the original surface. This fiber retraction resembles fiber slip and allows the fiber to reduce its stress level or to accept stress transfer more slowly. In contrast, a fixed displacement boundary condition reduces fiber retraction leading to higher local stress levels and to more rapid stress transfer. Because shear-lag analysis is not influenced by the details of the boundary conditions, it cannot predict the boundary condition effects. The shear-lag analysis presented here agrees much better with the uniform stress boundary conditions than it does with the fixed displacement boundary conditions. It might be possible to alter the basic shear-lag assumptions used here to develop a shear-lag analysis appropriate for fixed-end displacements. The result of such an analysis would be a new form for β. I am not aware of any attempts in the literature at a fixed axial displacement shear-lag analysis. Perhaps one should be derived before shear-lag analysis is used for analysis of fragmentation specimens.

5. Discussion

Shear-lag methods provide an approximate analytical tool for analysis of axisymmetric stress states in composites. The most basic shear-lag equations can be reduced to a set of second-order, ordinary differential equations with constant coefficients. The coefficients can be determined explicitly from exact elasticity equations by making a minimum of four assumptions. One possible set of four assumptions, which is consistent with most of the shear-lag literature, was discussed above.

For analysis of two concentric cylinders, the shear-lag equations reduce to a single, second-order differential equation with a single parameter β. In sample calculations, the shear-lag predictions for both average axial fiber stress and total strain energy agree within 20% with FEA calculations. The agreement holds over

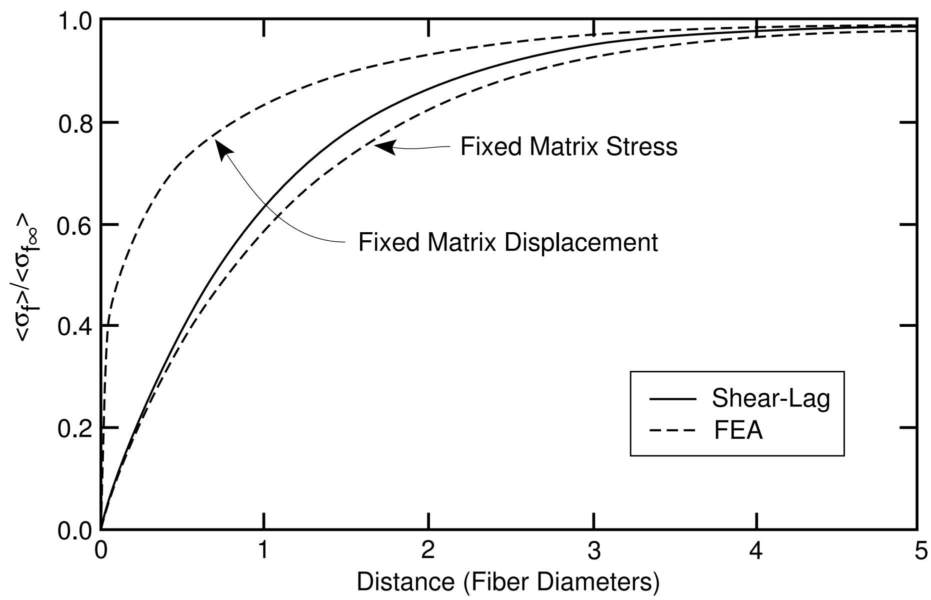

Fig. 6. The average axial fiber stress as a function of distance from the fiber break for $E_f/E_m = 10$ and $V_1 = 10\%$. The FEA analyses (dashed lines) are for either fixed displacement on uniform stress on the matrix ends. The shear-lag analysis in given by the solid line.

a wide range of fiber matrix modulus ratios, E_f/E_m, and fiber volume fractions, V_1. The errors generally increase as E_f/E_m decreases. Thus shear-lag analysis works best when the fiber is much stiffer than the matrix. Reasonable agreement with FEA calculations requires use of the β derived here and previously derived by Nayfeh (1977) and McCartney (1992). The shear-lag parameter proposed by Cox (1952) gives shear-lag predictions that are grossly in error with FEA calculations.

Shear-lag analysis does not work at low fiber volume fractions. The only recourse for shear lag analysis of a fiber in a large amount of matrix is to treat β as an unknown parameter. Perhaps β could be measured by comparison of shear-lag predictions to FEA calculations or by comparison to experimental results on stress transfer such as by Raman spectroscopy (Melanitis, Galiotis, Tetlow, and Davies, 1992). When β is treated as an adjustable parameter, or equivalently when the matrix is assumed to have an effective radius, the resulting shear-lag analysis should not be confused with true stress transfer analysis. By this approach, shear-lag analysis is simply representing the stresses as exponential in form. Because the exponential rate constants, which determine the stress transfer rate, are unknown, shear-lag analysis is giving no information about stress transfer rates.

Shear-lag analysis is often used to draw conclusions about the interfacial shear stress in composites. From the results in Fig. 1 the errors in shear stress are much larger than the errors in average axial stress. The larger errors in shear stress can be explained by Eq. (49). Interfacial shear stress is given by the z-derivative of average axial stress. Differentiation of approximate results always magnifies any errors. Thus the 10–20% errors in $\langle\sigma_f\rangle$ lead to 50–100% errors in interfacial shear stress. Furthermore, the shear stress errors depend on the specific values of E_f/E_m, V_1, and the distance from the fiber break. The interfacial shear stress errors may be positive or negative; in other words, the shear-lag predictions for interfacial shear stress may be either way too high or way too low.

The reasonable accuracy for total energy change (ΔU) suggests that shear-lag analysis might be useful in fracture mechanics analysis of single-fiber specimens. Most fracture mechanics methods, however, involve evaluating an energy release rate and not total energy. Like the shear stress-average axial stress relation, energy release rate is found by differentiating ΔU. Thus the 10–20% errors in ΔU should be expected to give very unreliable calculations for energy release rate. Is it doubtful that shear-lag analysis has sufficient accuracy for calculating energy release rates. An indirect fracture mechanics analysis of the fragmentation specimen has been proposed which considers not an energy release rate, but rather the damage caused by the total energy released when the fiber fractures (Wagner, Nairn, and Detassis, 1995). Such an analysis only uses ΔU and therefore shear-lag analysis is acceptable approach, albeit a qualitative one.

Some might argue that the shear-lag methods presented here can be improved by altering the four basic assumptions. Indeed, it might be possible, and even desirable, to alter the assumptions to suit various specific problems. The assumptions chosen here appear ideal for analysis of problems with uniform stress boundary conditions; a revised set of assumptions might give an optimal β for analysis of fixed displacement boundary conditions. But no set of assumptions will fundamentally alter the final form of the shear-lag equations. No set of assumptions can escape the fact that the shear-lag stresses are exponential in form while true stress transfer is nonexponential. The final assessment of an optimized shear-lag analysis for any specific problem will certainly be that it gives acceptable predictions for integrated results, like average axial stress or total strain energy, but that it gives unreliable predictions for shear stresses, transverse stresses, and energy release rates.

The questions remains — what analytical tools can be used when information not provided by shear-lag analysis is needed? There are some alternatives in the literature. Variational mechanics of stress transfer requires only one assumption — that that axial stresses in the fiber and matrix only weakly depend on r (Nairn,1992). Clearly such an analysis will improve on shear-lag methods, but it still has difficulties at low fiber volume fractions (Leroy, 1996). McCartney (1989, 1993) has derived alternate approximate elasticity equations for axisymmetric stress states. His analysis for two concentric cylinders (McCartney, 1989) appears mathematically equivalent to the variational mechanics analysis, but the elasticity techniques are more easily extended to multiple cylinders (McCartney, 1993) than are the variational techniques. Finally stress function analyses using infinite Bessel-Fourier series have been developed for both the pull-out test (Kurtz and Pagano, 1991) and the fragmentation test (Nairn, 1996). The suitability of these and possibly other analytical tools will be assessed in a future publication.

Acknowledgments

This work was supported, in part, by a grant from the Mechanics of Materials program at NSF (CMS-9401772), and , in part, by a grant from the United States-Israel Binational Science Foundation (BSF Grant No. 92-00170), Jerusalem, Israel. The author also acknowledges helpful discussions with Neil McCartney.

REFERENCES

Christenson, R. M. (1979), *Mechanics of Composite Materials*, John Wiley & Sons, New York.

Cox, H. L. (1952), The Elasticity and Strength of Paper and Other Fibrous Materials, *Brit. J. Appl. Phys. 3*, 72.

Feillard, P., G. Désermot, and J. P. Favre (1994), Theoretical Aspects of the Fragmentation Test, *Comp. Sci. & Tech. 50*, 265.

Hashin, Z. (1990), Thermoelastic Properties of Fiber Composites With Imperfect Interface, *Mech. of Materials 8*, 333.

Hseuh, C. H. (1988), Elastic Load Transfer From Partially Embedded Axially Loaded Fibre to Matrix, *J. Mat. Sci. Letts 7*, 497.

Hseuh, C. H. (1995), Modeling of Elastic Stress Transfer in Fiber-Reinforced Composites, *Trends in Polymer Science 10*, 336.

Jiang, K. R. and L. S. Penn (1992), Improved Analysis and Experimental Evaluation of the Single Filament Pull-Out Test, *Comp. Sci. and Tech. 45*, 89.

Kim, J. K., C. Baillie, and Y. M. Mai (1991), Interfacial Debonding and Fibre Pull-Out Stresses. Part I: Critical Comparison of Existing Theories, *J. Mat. Sci. 27*, 3143.

Kurtz, R. D. and Pagano, N. J. (1991), Analysis of the Deformation of a Symmetrically-Loaded Fiber Embedded in a Matrix Material, *Composites Engineering 1*, 13.

Lacroix, Th., B. Tilmans, R. Keunings, M. Desaeger, and I. Verpoest (1992), Modeling of Critical Fibre Length and Interfacial Debonding in the Fragmentation Testing of Polymer Composites, *Comp. Sci. & Tech. 43*, 379.

Lekhnitski, S. G. (1981), *Theory of an Anisotropic Body*, MIR Publishers, Moscow.

Leroy, F. H. (1996), On Analytical Approaches of the 3D Stress State in s Single Fibre Pull-Out Specimen, *J. Mat. Sci. Letts.*, submitted.

McCartney, L. N. (1989), New Theoretical Model of Stress Transfer Between Fibre and Matrix in a Uniaxially Fibre-Reinforced Composite, *Proc. R. Soc. Lond. A425*, 215.

McCartney, L. N. (1992), Analytical Models of Stress Transfer in Unidirectional Composites and Cross-Ply Laminates, and Their Application to the Prediction of Matrix/Transverse Cracking, *Local Mechanics Concepts for Composite Material Systems*, eds., J. N. Reddy and K. L Reifsnider, Proc. IUTAM Symposium, Blacksburg, VA, 1991, 251.

McCartney, L. N. (1993), Stress Transfer for Multiple Perfectly Bonded Concentric Cylinder Models of Unidirectional Composites, *National Physical Laboratory Report DMM(A)129*, Teddington, UK.

Melanitis, N., Galiotis, C., Tetlow, P. L. and Davies, C. K. L. (1992), Interfacial Shear Stress Distribution in Model Composites Part 2: Fragmentation Studies on Carbon Fibre/Epoxy Systems, *J. Comp. Mat. 26*, 574.

Nairn, J. A. (1992), A Variational Mechanics Analysis of the Stresses Around Breaks in Embedded Fibers, *Mech. of Materials 13*, 131.

Nairn, J. A. and Y. C. Liu (1996), Stress Transfer into a Fragmented, Anisotropic Fiber Through an Imperfect Interface, *Int. J. Solids Structures*, in press.

Nairn, J. A. and Y. C. Liu (1996), On the Use of Energy Methods for Interpretation of Results of Single-Fiber Fragmentation Experiments, *Composite Interfaces*, in press.

Nayfeh, A. H. (1977), Thermomechanically Induced Interfacial Stresses in Fibrous Composites, *Fibre Sci. & Tech. 10*, 195.

Piggott, M. R. (1987), Debonding and Friction at Fiber-Polymer Interfaces. I: Criteria for Failure and Sliding, *Comp. Sci. & Tech. 30*, 295.

Reissner, E. (1946), Analysis of Shear Lag in Box Beams by the Principle of Minimum Potential Energy, *Quart. Appl. Math. 4*, 268.

Troitsky, M. S. (1976), *Stiffened Plates: Bending, Stability and Vibrations*, Elsevier Scientific Publishing, Amsterdam.

Wadsworth, N. J. and I. Spilling (1968), Load Transfer from Broken Fibres in Composite Materials, *Br. J. Appl. Phys. (J. Phys. D.) 1*, 1049.

Wagner, H. D., J. A. Nairn, and M. Detassis (1995), Toughness of Interfaces from Initial Fiber-Matrix Debonding in a Single-Fiber Composite Fragmentation Test, *Applied Comp. Mater. 2*, 107.